Ultra-Wideband Circular Microstrip Antenna with Hybrid EBG for reduced SAR

Mahesh M. Munde, Anil B. Nandgaonkar, and Shankar B. Deosarkar

Department of Electronics and Telecommunication Engineering, Dr. Babasaheb Ambedkar Technological University, Lonere-402103, Maharashtra, India

Corresponding author: Mahesh M. Munde (e-mail: maheshmunde79@ gmail.com).

ABSTRACT This article presents a basic ultra-wideband circular microstrip antenna (UWB-CMSA) with partial ground resonating from 2.38 GHz to 12 GHz for handheld devices. The designed antenna covers bands for Bluetooth (2.4 GHz), LTE (2.5/2.69 GHz), WLAN (2.4/3.5/5 GHz), and WiMAX (2.5/3.5/5.5) GHz applications. Specific Absorption Rate (SAR) values of certain bands exceed the limit for UWB-CMSA. A uniplanar spiral unit cell is designed and exhibits phase reversal for 2.4 GHz, 3.5 GHz, and 5.5 GHz. EBG unit cells are placed near the feed for surface wave minimization to achieve a reduction in SAR. Furthermore, the EBG structure is placed on the ground plane to analyse the impact, also designs are fabricated, and results are compared. Mushroom type M-shaped unit cell is designed which offers phase reversal at 2.3 GHz which is placed near feed in a similar fashion to the earlier spiral one to suppress surface waves also the structure is investigated by arranging it on a ground plane. SAR is reduced for all the cases being inspected but for certain bands it exceeds the limit of 1.6 W/kg. A combination of two different unit cells to form a hybrid EBG structure is proposed and evaluated by placing it near the feed. SAR is curtailed by 87.05% at 5.5 GHz.

INDEX TERMS CMSA, EBG, Hybrid, M-shaped, SAR, Spiral, UWB.

I. INTRODUCTION

Nowdays, wireless communication systems operate at multiple bands, and to enhance data rates, we need systems that will operate over wideband and such systems essentially utilize multiband, wideband, and ultra-wideband (UWB) antennas to accommodate multiple applications. To make the antenna system cost-effective it must use a multiband antenna or UWB antenna, which can be integrated with a communication system, so they serve the purpose. Wireless devices which are operated close to humans, implantable devices, and body worn devices emit radio frequency (RF) radiations besides the human body being lossy, absorbs radiations, and heating of the tissues occurs. Various harmful effects of RF radiation on humans and safety issues are listed in [1]. Specific absorption rate (SAR) is a metric to estimate the amount of RF energy absorbed by the human tissue and various methods for SAR reduction are reviewed in [2].

Various regular shapes of printed monopole antennas with feed at different positions and of different lengths for UWB applications are presented in [3]. Two monopole antennas are combined to cover UWB applications [4]. An analysis on the placement of open-loop-ring-resonator as parasitic element with monopole antenna for enhancement of impedance bandwidth is proposed in [5]. A U-shaped monopole antenna with an 8-shaped slot on the patch and ground to achieve broadband circular polarization is presented in [6]. Slot in antenna and parasitic element are investigated for the widening of a continuous band and gain improvement in [7].

Electromagnetic band gap (EBG) structures with UWB monopole antenna are used to achieve notches in specific bands by offering stop band features at WLAN and Wi-MAX for rejecting these bands are proposed in [8][9], also EBG structures are used as superstrates for a reduction in surface waves and SAR [10][11]. Phase reflection property and characterization of high impedance surfaces are evaluated in [12-14]. [15][16] investigated removal of surface waves and performance improvement by using EBG structures. Safety guidelines and limits for radio frequency exposure are quoted in [17][18].

In this article, section II presents a basic configuration of circular microstrip antenna for UWB applications in wireless systems and SAR estimation. Section III presents spiral uniplanar and M-shaped mushroom type EBG along with antenna and modeling of a spiral unit cell. Placement of unit cells is carried out in two different ways first near the feed and second on a ground plane, SAR is estimated for different placements. Section IV presents the placement of a combination of spiral and M-shaped unit cells near the feed

of the antenna to form a hybrid EBG structure. Section V presents conclusions.

II. DESIGN AND ANALYSIS OF UWB-CMSA

The basic antenna structure is designed using equations refer from 1 to 5 and is shown in Fig. 1, fabricated on FR-4 material with a dielectric constant of 4.3, loss tangent 0.025, and substrate thickness of 1.6 mm and is depicted in Fig. 2. The configuration of CMSA designed operates over UWB from 2.4 GHz to 12 GHz so can accommodate all major applications for handheld devices and serves as a basic geometry for extended structures [3][19]. The frequency bands of interest are 2.4 GHz which accommodates Bluetooth, and Wi-Fi, 3.5 GHz which accommodates WiMAX and 5/6 GHz are used for Wi-Fi.

$$F_{mn} = \left(\frac{CX_{mn}}{2\pi r\sqrt{\varepsilon_{eff}}}\right) \quad (1)$$

where F_{mn} is resonant frequency, c is speed of light in free space, X_{mn} is first order Bessel function root, r is radius of the patch, ε_{eff} is effective dielectric constant.

In circular antenna, TM_{11} mode is dominant and is given refer to (4), for ε_{eff} refers to (2). Equation (3) gives effective radius (r_e) considered due to fringing fields [19][20]. Equation (5) gives the width of the feed.

$$\varepsilon_{eff} = \left(\frac{\varepsilon_r+1}{2}\right) + \left(\frac{\varepsilon_r-1}{2}\right)\left(1+\frac{12h}{w}\right)^{-\frac{1}{2}} \quad (2)$$

$$r_e = r\left(1+\frac{2h}{\pi r\varepsilon_r}\left(ln\left(\frac{\pi r}{2h}\right)+1.7726\right)\right)^{\frac{1}{2}} \quad (3)$$

$$F_{mn} = \left(\frac{1.8412\,C}{2\pi r_e\sqrt{\varepsilon_{eff}}}\right) \quad (4)$$

$$w_f = \frac{7.48h}{e^{\left(\frac{z_0\sqrt{\varepsilon_r}+1.41}{87}\right)}} - 1.25t \quad (5)$$

where ε_r is relative permittivity, h is substrate height, w is width, z_0 is single ended impedance, and t is trace thickness.

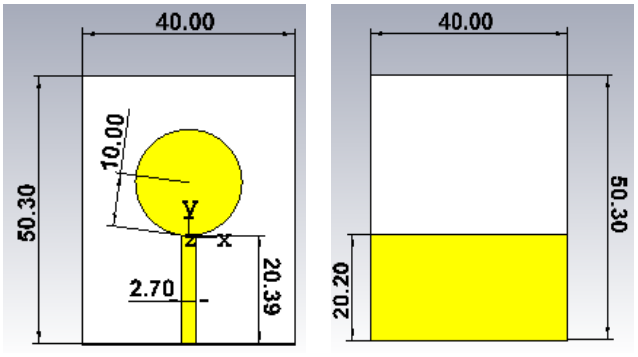

FIGURE 1. Designed UWB-CMSA. All dimensions depicted in the figure are in mm.

Fig. 3 represents simulated and measured results for UWB-CMSA which are in close agreement over the entire band i.e., return loss of 10 dB is achieved over the range of 2.37 GHz to 11.95 GHz. First resonance occurs at 3.91 GHz with the return loss of 25.23 dB and second resonance at 9.37 GHz with a return loss of 53.90 dB. Fig. 4 reveals impedance matching for the desired band. Fig. 5 reveals the maximum value of gain over the entire band from 2.37 GHz to 11.95 GHz. Gain varies from 1.388 dB at 4.8 GHz to 5.19 dB at 9.6 GHz.

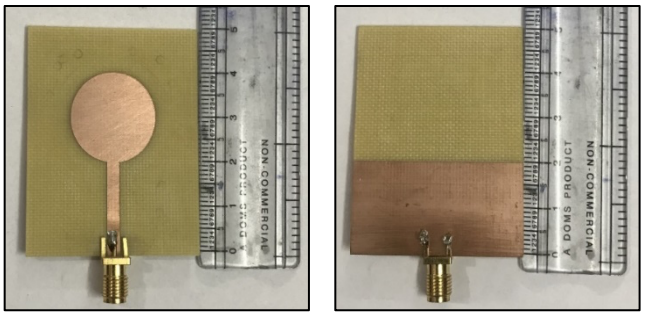

Figure 2. Fabricated UWB-CMSA.

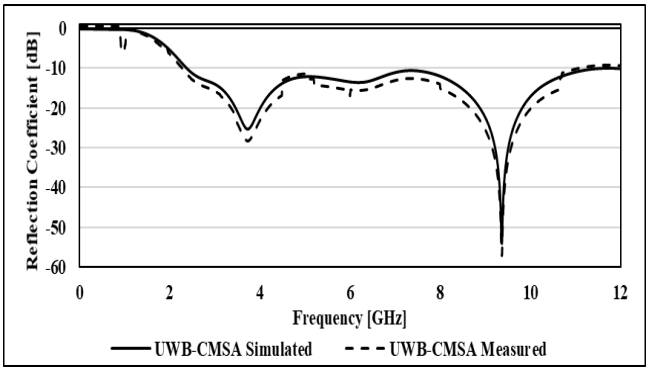

Figure 3. Reflection Coefficient v/s Frequency for UWB-CMSA.

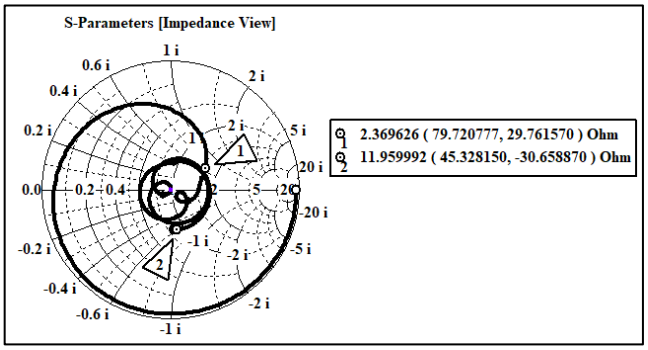

Figure 4. Variation in Impedance v/s frequency.

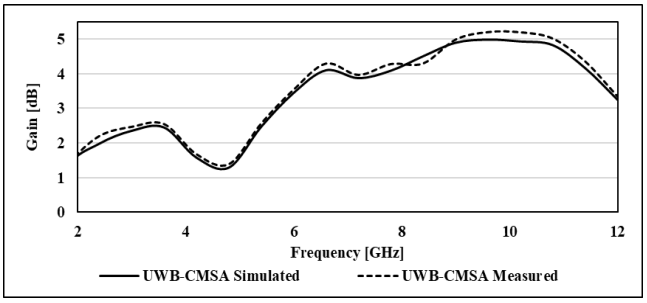

Figure 5. Variation in maximum gain v/s frequency.

Fig. 6 reveals radiation efficiency is more than 70% as it indicates power losses in a dielectric substrate and metal along with accepted and radiated power on which radiation efficiency is dependent, also SAR is dependent on losses in substrate and metal, so losses should be minimum to keep SAR minimum but as frequency is increasing losses are increasing which is evident from Fig. 6. Fig. 7 (a), (b), (c) shows directivity at desired frequencies.

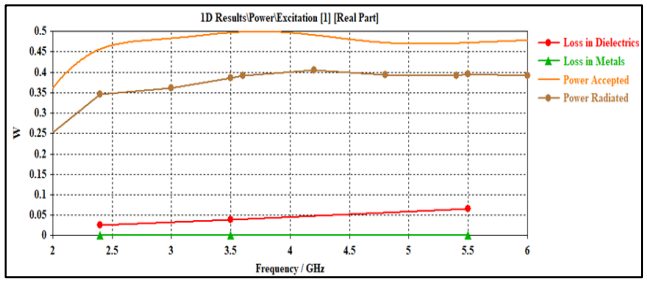

Figure 6. Power loss curve v/s frequency.

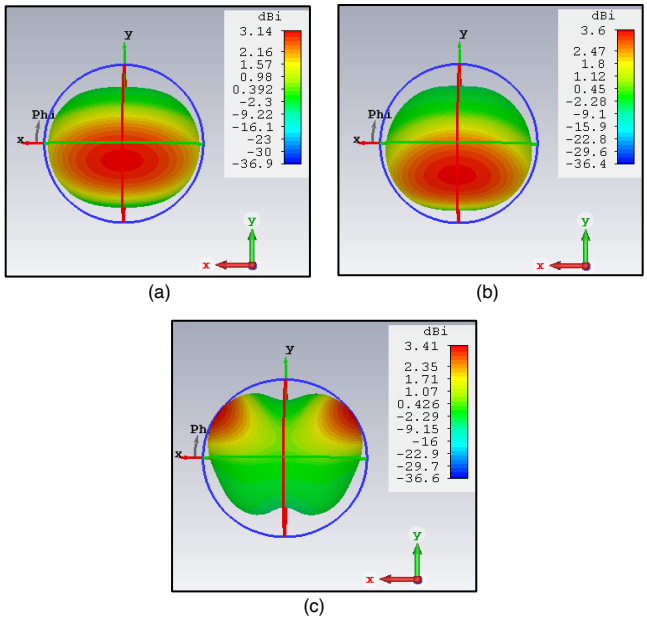

Figure 7. Directivity in dBi at (a) 2.4 GHz (b) 3.5 GHz (c) 5.5 GHz.

Fig. 8 (a) and (b) reveal the radiation patterns for XZ and YZ plane of UWB-CMSA. UWB antennas are operated over a large range of frequencies and support different applications but when used for the mobile handsets they must comply with the guidelines given by FCC and IEEE C95.3. Fig. 9 (a), (b), (c) depicts SAR values for 1 gram of tissue mass. SAR values for frequency bands of 3.5 GHz and 5.5 GHz are extremely high and needs to be minimized so that it will be within limits specified by IEEE and FCC. Dielectric properties of tissues of SAM phantom head model are frequency-dependent and used from [21] for 2.4 GHz, 3.5 GHz, and 5.5 GHz.

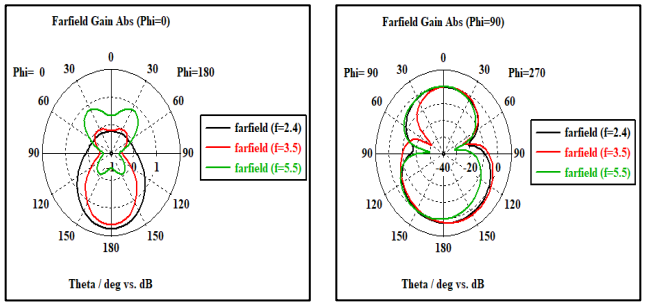

Figure 8. Radiation pattern of UWB-CMSA (a) XZ plane (b) YZ plane.

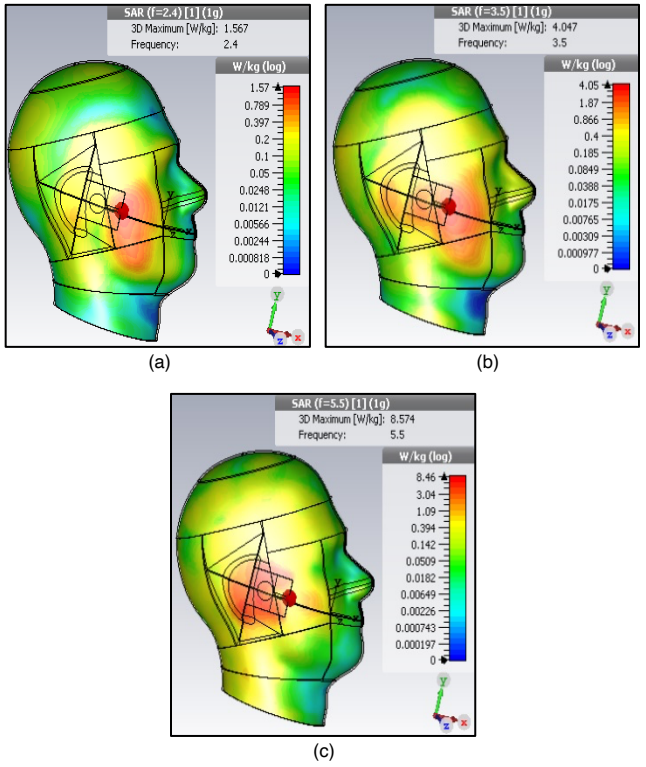

Figure 9. SAR for UWB-CMSA at (a) 2.4 GHz (b) 3.5 GHz (c) 5.5 GHz.

III. DESIGN AND ANALYSIS OF UWB-CMSA WITH SPIRAL AND M-SHAPED EBG NEAR FEED

According to the surface current distribution at 2.4 GHz, feed gives spurious radiation due to which surface waves are generated. These waves are contributing to losses in the substrate and will increase SAR value. Spiral EBG and M-shaped EBG unit cells are placed on both sides of the feed of the basic configuration depicted in Fig. 1 to minimize SAR. TM and TE surface waves propagate if surface impedances are inductive and capacitive respectively. The zero-phase on impedance plot of unit cells indicates very high impedance is offered and will not allow surface waves to propagate through the structure.

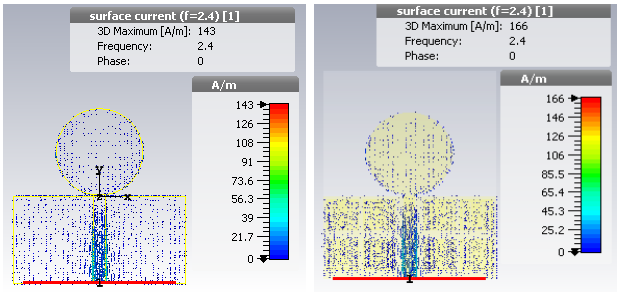

Figure 11. Surface current at 2.4 GHz for CMSA with and without EBG.

Fig. 10 gives the designed EBG unit cell [22] along with dimensions in mm and Fig. 11 (a) and (b) shows analysis of unit cell for phase reversal using transmission line (suspended line) method [12]. It is one of the simplest and accurate method which utilizes the transmission line above the unit cell to analyze and plot phase reversal characteristics of the EBG unit cell. One end of the transmission line is connected to port 1 and another end to port 2 that collects the current passing through a transmission line. The EBG unit cell placed above will exhibit a slow wave effect and causes phase reversal of the wave. Fig. 12 reveals a plot of S-parameter phase in degrees in the range of ±180 versus frequency. Fig. 13 and Fig. 14 show the designed and fabricated top and bottom views of UWB-CMSA with spiral EBG. Placement and location of EBG unit cells are chosen by performing parametric analysis in simulation tool for the smallest value of SAR.

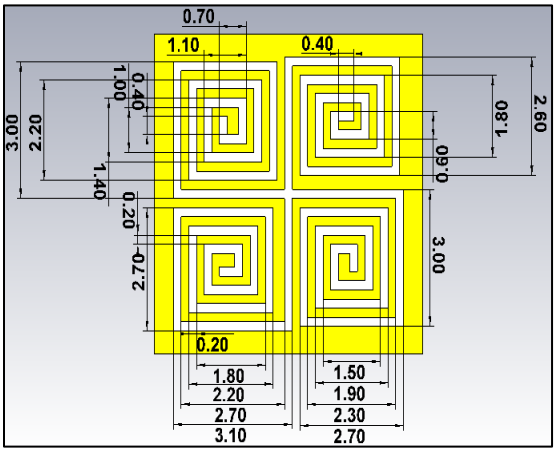

Figure 10. Designed spiral EBG unit cell.

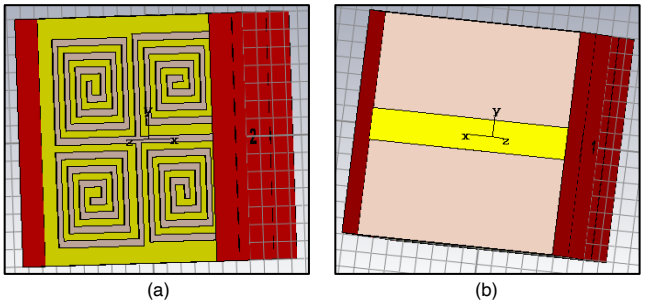

Figure 11. Spiral EBG unit cell simulation using suspended line method with wave ports (a) Top view (b) Bottom view

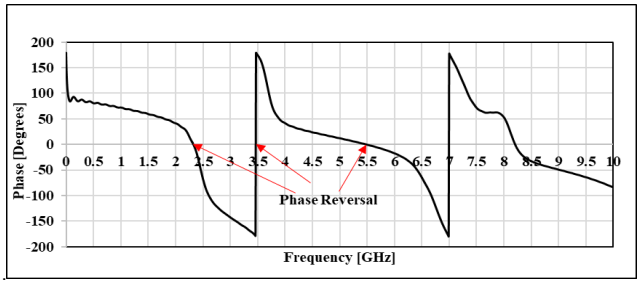

Figure 12. Reflection parameter (S_{11}) of a unit cell in degrees for phase reversal.

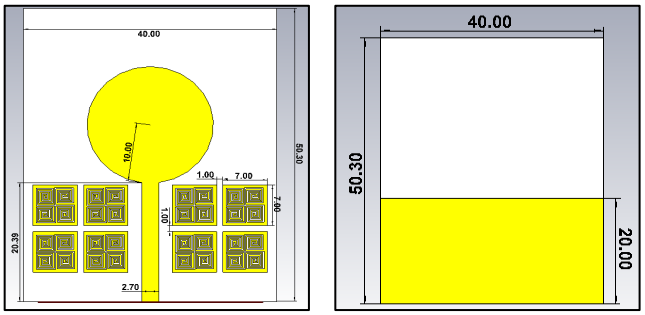

Figure 13. Designed UWB-CMSA with spiral EBG near the feed.

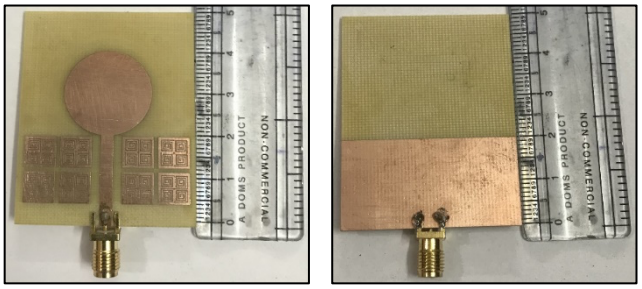

Figure 14. Fabricated UWB-CMSA with spiral EBG near feed.

Fig. 15 and Fig. 16 shows a designed and fabricated prototype of UWB-CMSA with M-shaped EBG unit cells placed near feed to eliminate spurious radiations from the feed and minimize surface waves to reduce SAR. Fig. 17 reveals a comparison of return loss > 10 dB for the antenna with spiral EBG and M-shaped EBG. Simulated and measured return loss characteristics are in close agreement for lower frequencies whereas some deviations are observed at higher frequencies due to variations in capacitance for different EBG structures as the path length of microstrip varies [22].

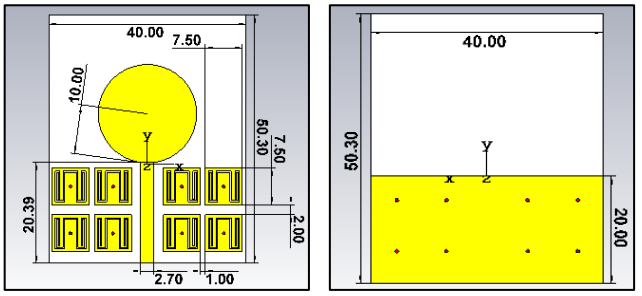

Figure 15. Designed UWB-CMSA with M-shaped EBG near the feed.

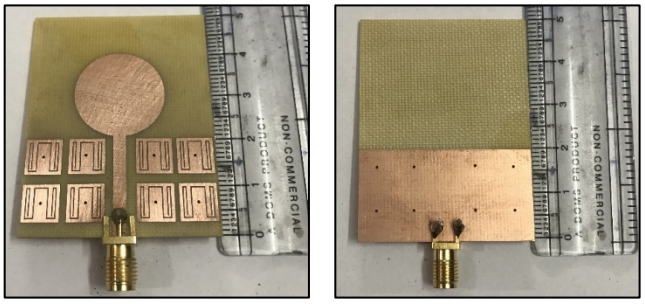

Figure 16. Designed UWB-CMSA with M-shaped EBG near the feed.

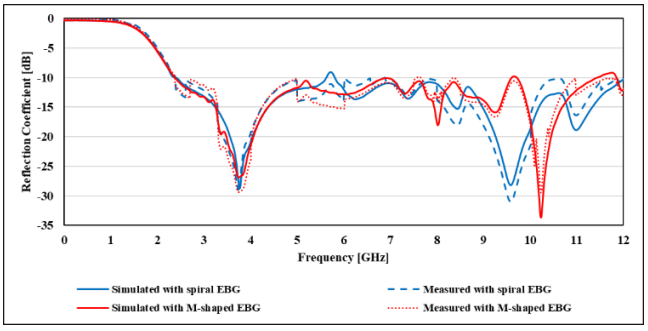

Figure 17. Variation in S-parameter v/s frequency for spiral and M-shaped EBG near feed.

SAR values for 1 gram tissue mass aimed at UWB-CMSA, UWB-CMSA with spiral EBG unit cells, and UWB-CMSA with M-shaped EBG unit cells are compared in Table I.

TABLE I. Comparison of SAR [W/Kg] in 1 gram tissue mass

Frequency [GHz]	UWB-CMSA	UWB-CMSA with spiral EBG	UWB-CMSA with M-shaped EBG
2.4	1.567	0.406	0.443
3.5	4.047	2.516	1.947
5.5	8.574	4.407	3.503

SAR reduction achieved using EBG reported in the literature is 24% in [23] at 1900 MHz, 95% in [24] at 2.4 GHz, 76.37 % at 10 gram of tissue mass in [25] at 2.5 GHz. SAR reduction achieved in this work at 2.4 GHz is 74.09% and 71.72%, at 3.5 GHz is 37.83% and 51.89%, at 5.5 GHz is 48.60 and 59.14% for UWB-CMSA with spiral and M-shaped EBG respectively, but for the wireless handheld devices operated near the head must comply with the FCC standard and SAR should be less than 1.6 W/Kg in 1 g tissue mass.

IV. ANALYSIS OF UWB-CMSA WITH HYBRID EBG NEAR FEED

A novel approach of using a combination of two different EBG structures one as a uniplanar spiral EBG and another as mushroom type M-shape EBG is explored for SAR reduction. Uniplanar spiral EBG gives phase reversal for all the bands whereas mushroom type M-shape EBG will divert surface waves to ground through via and back to the top layer for radiation due to phase reflection property of EBG thereby reducing back lobes.

Fig. 18 and Fig. 19 depict designed and fabricated prototypes of UWB-CMSA with hybrid EBG unit cells placed near feed to reduce spurious radiations from a feed. Spiral EBG unit cells, when placed near feed, acts as a parasitic element, to achieve the band stop feature of spiral EBG unit cells they are placed away from feed, and mushroom type are placed close to the feed.

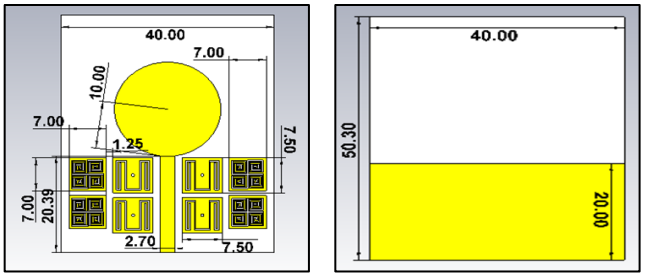

Figure 18. Designed UWB-CMSA with hybrid EBG near the feed.

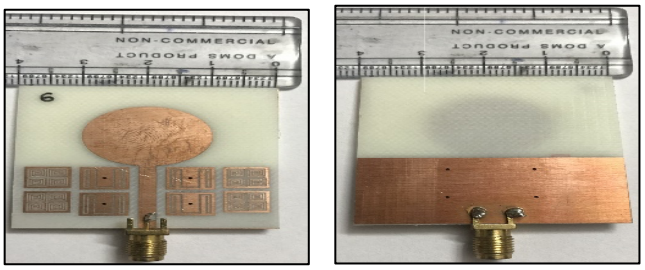

Figure 19. Fabricated UWB-CMSA with hybrid EBG near feed.

Fig. 20 shows the reflection coefficient over the band covering from 2.38 GHz to 12 GHz and the entire band depicted gives a better impedance match for simulated and measured results.

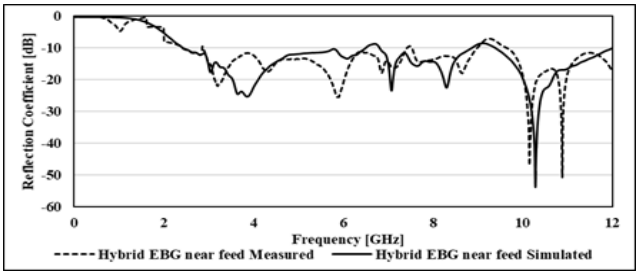

Figure 20. Variation in S-parameter vs frequency for UWB-CMSA with hybrid EBG.

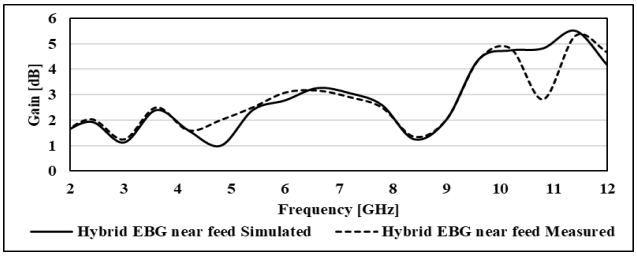

Figure 21. Variation in maximum gain vs frequency for UWB-CMSA with hybrid EBG.

Fig. 21 reveals simulated and measured gain over the entire band, minimum value of gain is 1.00 dB at 4.8 GHz and maximum value of 5.3 dB at 11.4 GHz. Fig. 22 shows combined radiation patterns at phi 0 and phi 90 for 2.4 GHz, 3.5 GHz, and 5.5 GHz, and is evident that backward radiation is suppressed more when compared with previous designs and is responsible for SAR reduction to some extent.

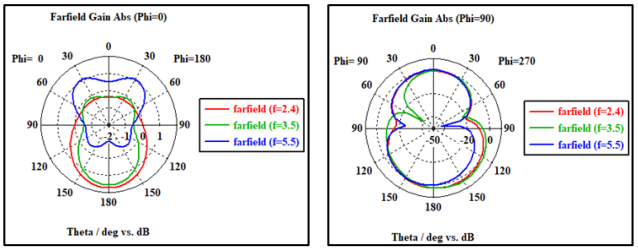

(a) (b)

Figure 22. Radiation pattern of UWB-CMSA with hybrid EBG (a) XZ plane (b) YZ plane

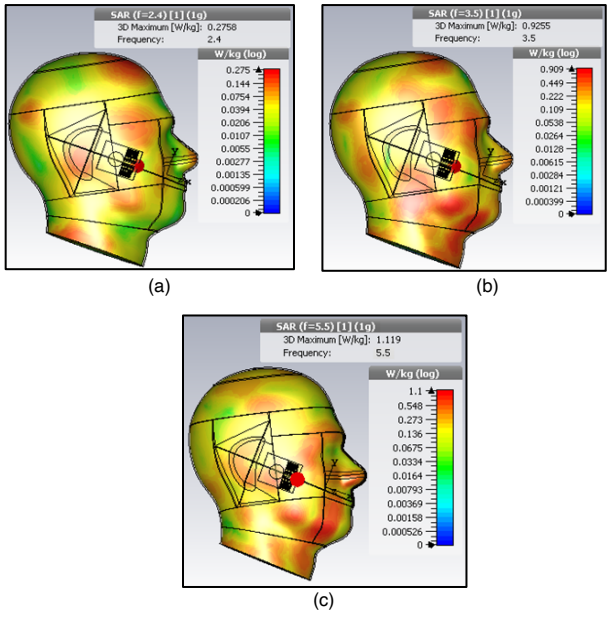

(a) (b)

(c)

Figure 23. SAR for UWB-CMSA with hybrid EBG at (a) 2.4 GHz (b) 3.5 GHz (c) 5.5 GHz.

From Fig. 23 (a), (b), and (c) it is evident that values of SAR in 1 gram of tissue mass at 2.4 GHz, 3.5 GHz, and 5.5 GHz respectively are minimal when compared with the above designs, SAR is certainly reduced by 82.39% at 2.4 GHz, 77.13% at 3.5 GHz, and 87.05% at 5.5 GHz and percentage reduction and comparison is depicted in Table II.

TABLE II. Comparison of SAR [W/Kg] for UWB-CMSA with and without hybrid EBG in 1 gram tissue mass

Frequency [GHz]	UWB-CMSA	UWB-CMSA with hybrid EBG	% reduction
2.4	1.567	0.2758	82.39
3.5	4.047	0.9255	77.13
5.5	8.574	1.11	87.05

V. CONCLUSION

UWB-CMSA with the partial ground is designed and fabricated as a basic configuration but SAR is well above limits specified by FCC and IEEE for 3.5 GHz and 5.5 GHz and is 1.567 W/Kg for 2.4 GHz. Uniplanar spiral EBG when used near feed reduces SAR at all bands but is not within limits for 3.5 GHz and 5.5 GHz. Mushroom type M-shape EBG when used near feed reduces SAR at all bands but is not within limits for 3.5 GHz and 5.5 GHz, besides is less for 5.5 GHz than UWB-CMSA and UWB-CMSA with uniplanar spiral EBG structure. From the above observations and analysis of spiral and M-type, a combination of spiral and M-shape has given rise to a hybrid type of EBG structure. By using a hybrid type of EBG structure, it is distinct from SAR values in tables I and II that hybrid EBG structure reduces SAR to a maximum extent and is well within limits specified by IEEE and FCC.

REFERENCES

[1] M. Munde, G. Fernando, N. Fernandes, A. Gurav and A. Nandgaonkar, "ANDLINE: A simple solution for the cons of using a mobile phone," 2015 IEEE UP Section Conference on Electrical Computer and Electronics (UPCON), Allahabad, India, 2015, pp. 1-5, doi: 10.1109/UPCON.2015.7456701.

[2] R. Pikale, D. Sangani, P. Chaturvedi, A. Soni and M. Munde, "A Review: Methods to Lower Specific Absorption Rate for Mobile Phones," 2018 International Conference on Advances in Communication and Computing Technology (ICACCT), Sangamner, India, 2018, pp. 340-343, doi: 10.1109/ICACCT.2018.8529654.

[3] K. P. Ray, "Design Aspects of Printed Monopole Antennas for Ultra-Wide Band Applications", *International Journal of Antennas and Propagation*, vol. 2008, Article ID 713858, 8 pages, 2008, https://doi.org/10.1155/2008/713858.

[4] Kumar, P., & Masa-Campos, J. L. (2016). Dual Polarized Monopole Patch Antennas for UWB Applications with Elimination of WLAN Signals. *Advanced Electromagnetics*, *5*(1), 46-52, https://doi.org/10.7716/aem. v5i1.305.

[5] Boutejdar, A., Challal, M., Bennani, S., Mouhouche, F., & Djafri, K. (2017). Design and Fabrication of a Novel Quadruple-Band Monopole Antenna Using a U-DGS and Open-Loop-Ring Resonators. *Advanced Electromagnetics*, *6*(3), 59-63, https://doi.org/10.7716/aem.v6i3.573.

[6] Jangid, K., Jain, P., Sharma, B., Saxena, V., Kulhar, V., & Bhatnagar, D. (2017). Ring Slotted Circularly Polarized U-Shaped Printed Monopole Antenna for Various Wireless Applications. Advanced Electromagnetics, 6(1), 70-76, https://doi.org/10.7716/aem.v6i1.460.

[7] T. Alam, M. Faruque and M. Islam, "Printed circular patch wideband antenna for wireless communication," Informacije Midem Journal of Microelectronics Electronic Components and Materials, vol. 44, pp. 212–217, 2014.

[8] L. Peng and C. Ruan, "UWB Band-Notched Monopole Antenna Design Using Electromagnetic-Bandgap Structures," in *IEEE Transactions on Microwave Theory and Techniques,* vol. 59, no. 4, pp. 1074-1081, April 2011, doi: 10.1109/TMTT.2011.2114090.

[9] Hao Liu, Ziqiang Xu, "Design of UWB Monopole Antenna with Dual Notched Bands Using One Modified Electromagnetic-Bandgap Structure", *The Scientific World Journal*, vol. 2013,

Article ID 917965, 9 pages, 2013, https://doi.org/10.1155/2013/917965.

[10] Mahesh Munde, Anil Nandgaonkar, and Shankar Deosarkar, "Dual Feed Wideband Annular Ring Microstrip Antenna with Circular DGS for Reduced SAR," Progress In Electromagnetics Research B, Vol. 88, 175-195, 2020, https://doi:10.2528/PIERB20071804.

[11] Mahesh Munde, Anil Nandgaonkar, and Shankar Deosarkar, "Low Specific Absorption Rate Antenna Using Electromagnetic Band Gap Structure for Long Term Evolution Band 3 Application," Progress In Electromagnetics Research M, Vol. 80, 23-34, 2019, https://doi:10.2528/PIERM18102103.

[12] Zhu, Y., Bossavit, A. & Zouhdi, S. Surface impedance models for high impedance surfaces. Appl. Phys. A 103, 677–683 (2011). https://doi.org/10.1007/s00339-010-6201-3.

[13] J. Sarrazin, A. Lepage and X. Begaud, "Circular High-Impedance Surfaces Characterization," in IEEE Antennas and Wireless Propagation Letters, vol. 11, pp. 260-263, 2012, doi: 10.1109/LAWP.2012.2189349.

[14] F. Linot, R. Cousin, X. Begaud and M. Soiron, "Design and measurement of High Impedance Surface," Proceedings of the Fourth European Conference on Antennas and Propagation, Barcelona, 2010, pp. 1-4.

[15] F. Yang and Y. Rahmat-Samii, "Reflection phase characterization of an electromagnetic band-gap (EBG) surface," IEEE Antennas and Propagation Society International Symposium), San Antonio, pp. 744-747, 2002.

[16] F. Yang and Y. Rahmat-Samii, "Electromagnetic Band Gap Structures in Antenna Engineering," New York, Cambridge University Press, 2009.

[17] Institute of Electrical and Electronic Engineers (IEEE), IEEE C95.1-2005, "Standards for Safety Levels with Respect to Human Exposure to Radio Frequency Electromagnetic Fields," IEEE Press, New York 2005.

[18] International commission on Non-Ionizing Radiation Protection (ICNIRP), "Guidelines for Limiting Exposure to Time-Varying Electric, Magnetic, and Electromagnetic Fields (Up to 300 GHz)," Health physics, vol. 74, pp. 494-522, 1998.

[19] Ramesh Garg, "Microstrip antenna design handbook," Boston, Artech House, 2001.

[20] Constantine Balanis, "Antenna Theory: Analysis and Design," New-Delhi, Wiley India, Reprint, 2016.

[21] ITIS Foundation, "Dielectric properties of body tissues," https://itis.swiss/virtual-population/tissue-properties/database/dielectric-properties.

[22] Q. Zheng, Y. Fu and N. Yuan, "A Novel Compact Spiral Electromagnetic Band-Gap (EBG) Structure," in *IEEE Transactions on Antennas and Propagation*, vol. 56, no. 6, pp. 1656-1660, June 2008, doi: 10.1109/TAP.2008.923305.

[23] R. Das and H. Yoo, "Application of a Compact Electromagnetic Bandgap Array in a Phone Case for Suppression of Mobile Phone Radiation Exposure," in *IEEE Transactions on Microwave Theory and Techniques*, vol. 66, no. 5, pp. 2363-2372, May 2018, doi: 10.1109/TMTT.2017.2786287.

[24] Ashyap AYI, Elamin NIM, Dahlan SH, Abidin ZZ, See CH, Majid HA, et al. (2021) Via-less electromagnetic band-gap-enabled antenna based on textile material for wearable applications. PLoS ONE 16(1): e0246057. doi.org/10.1371/journal.pone.0246057.

[25] K. Rao, P. Rao and V. Sumalatha, "Checkerboard Electromagnetic Band Gap (EBG) Structured S-Shaped Antenna for Wearable Applications," *Journal of Critical Reviews*, vol. 7, no. 4, pp. 621-631, Feb. 2020, dx.doi.org/10.31838/jcr.07.04.115.